

# Scattering in complex geometrical optics and the inverse problem for the conductivity equation

Matti Lassas

University of Helsinki

In collaboration with

Allan Greenleaf

Matteo Santacesaria

Samuli Siltanen

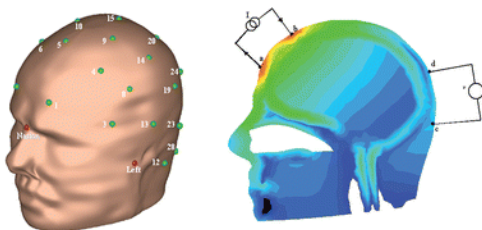
Gunther Uhlmann



Finnish Centre of Excellence  
in Inverse Problems Research

## Outline:

- ▶ Inverse conductivity problem
- ▶ Motivation of the edge detection problem
- ▶ Complex principal type operators
- ▶ Beltrami equation
- ▶ Single scattering and connection to Radon transform
- ▶ Analysis of higher order terms



# Inverse problem for the conductivity equation

## Conductivity equation

$$\nabla \cdot \sigma(x) \nabla u(x) = 0 \quad \text{on } \Omega \subset \mathbb{R}^d, \quad d = 2.$$

**Inverse problem:** Do the measurements made on the boundary determine the conductivity, that is, does the voltage-to-current map or the **Dirichlet-to-Neumann operator**  $\Lambda_\sigma$ ,

$$\Lambda_\sigma : u|_{\partial\Omega} \mapsto \nu \cdot \sigma \nabla u|_{\partial\Omega}$$

determine the conductivity  $\sigma(x)$  in  $\Omega$ ?

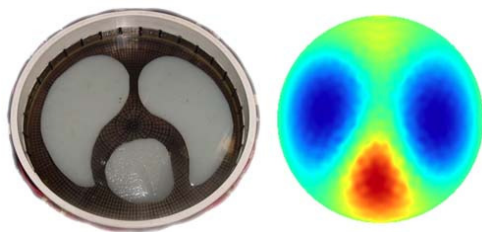


Figure: EIT by Isaacson, Mueller, Newell and Siltanen.

## Some results on the Electrical Impedance Tomography (EIT)

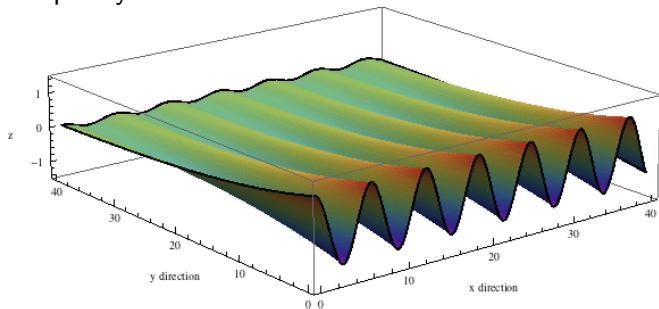
- ▶ Calderón 1980: Linearized problem.
- ▶ Sylvester-Uhlmann 1987, Nachman 1988: Smooth conductivities in 3D.
- ▶ Nachman 1996: Smooth conductivities in 2D.
- ▶ Isaacson-Mueller-Newell-Siltanen 2004: Numerical reconstruction algorithm.
- ▶ Astala-Päivärinta 2006: Bounded conductivities in 2D, Astala-L.-Päivärinta 2016: Degenerated conductivities in 2D.
- ▶ Lee-Uhlmann 1989, L.-Uhlmann 2001, L.-Taylor-Uhlmann 2003, Dos Santos Ferreira-Kenig-Salo-Uhlmann 2009: Inverse problem for  $\Delta_g$  on manifolds.
- ▶ Greenleaf-L.-Uhlmann 2003: Counterexamples related to invisibility cloaking.
- ▶ Daude-Kamran-Nicoleau 2016: New counterexamples with smooth conductivities.

## Exponentially decaying waves

Let  $\xi = (a, ib) \in \mathbb{C}^2$  where  $a, b \in \mathbb{R}$ ,  $|a| = |b|$ , and  $b > 0$ . Then

$$u(x) = e^{i\xi \cdot x} = e^{iax_1} \cdot e^{-bx_2}, \quad x = (x_1, x_2) \in \mathbb{R} \times \mathbb{R}_+$$

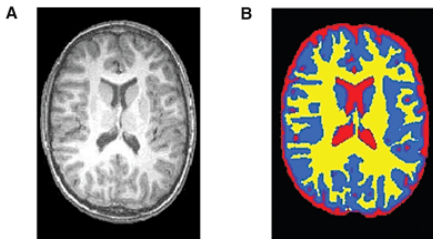
are solutions of  $\nabla \cdot \nabla u(x) = 0$  in the half-space  $\mathbb{R} \times \mathbb{R}_+$ . These solutions decay as  $x_2 \rightarrow \infty$  and oscillate in the  $x_1$  direction with the spatial frequency  $a$ .



The vector  $\xi \in \mathbb{C}^2$  is called the **complex wave number** or the **complex frequency** and  $u$  a solution of **Complex Geometrical Optics**.

## Outline:

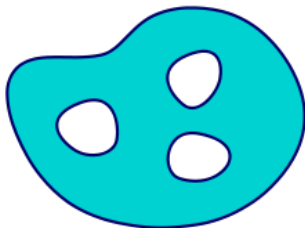
- ▶ Inverse conductivity problem
- ▶ Motivation of the edge detection problem
- ▶ Complex principal type operators
- ▶ Beltrami equation
- ▶ Single scattering and connection to Radon transform
- ▶ Analysis of higher order terms



# Edge detection in Electric Impedance Tomography

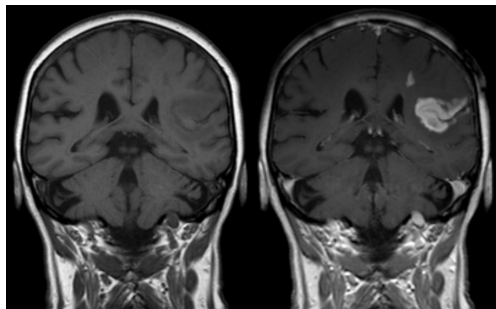
Our aim in this talk is to determine jumps of the conductivity function.

In particular, we want to determine locations of several jump surfaces in the presence of smooth, unknown background conductivity.



# Why a new edge detection method?

Our main motivation: **brain strokes imaging**.



- **ischemic stroke: lower conductivity.**  
Left: MRI image of ischemia (Hellerhoff 2010)
- **haemorrhagic stroke: higher conductivity.**

Challenges:

- low conductive skull layer,
- unknown background.

Some existing work:

- (Shi et al, 2009) experimental study on rhesus monkeys,
- (Malone et al., 2014) simulated multi-frequency data.



## Outline:

- ▶ Inverse conductivity problem
- ▶ Motivation of the edge detection problem
- ▶ Complex principal type operators
- ▶ Beltrami equation
- ▶ Single scattering and connection to Radon transform
- ▶ Analysis of higher order terms

$$\{p_R, p_I\} = 0$$

# Solutions in complex geometrical optics

Let  $\Omega = B(0, 1) \subset \mathbb{R}^2$  and

$$\begin{aligned}\sigma &: \mathbb{R}^2 \rightarrow \mathbb{R}, \\ 0 &< c_0 \leq \sigma(x) \leq c_1, \\ \text{supp}(\sigma) &\subset \Omega.\end{aligned}$$

Let us consider

$$\nabla \cdot (\sigma(x) \nabla u(x)) = 0, \quad x = (x_1, x_2) \in \mathbb{R}^2. \quad (1)$$

Let

$$\eta = \eta_R + i\eta_I \in \mathbb{C}^2 \text{ with } |\eta_R| = |\eta_I| \text{ and } \tau \in \mathbb{R}.$$

We consider solutions of (1) of the form

$$u(x) = e^{i\tau\eta \cdot x} v(x, \tau).$$

Since  $u(x) = e^{i\tau\eta \cdot x} v(x, \tau)$  satisfies the conductivity equation,

$$\begin{aligned} 0 &= \frac{1}{\sigma(x)} \nabla \cdot (\sigma(x) \nabla u(x)) \\ &= \left( \Delta + \frac{1}{\sigma} (\nabla \sigma) \cdot \nabla \right) (e^{i\tau\eta \cdot x} v(x, \tau)) \\ &= \left( \Delta v(x, \tau) + 2i\tau\eta \cdot \nabla v(x, \tau) + \left( \frac{1}{\sigma} \nabla \sigma \right) \cdot (\nabla + i\tau\eta) v(x, \tau) \right) e^{i\tau\eta \cdot x} \end{aligned}$$

## Equation in time-domain

Let  $\widehat{v}(x, t) = \mathcal{F}_{\tau \rightarrow t}(v(x, \tau))$  be the Fourier transform of  $v(x, \tau)$  in the  $\tau$  variable, that is,

$$\widehat{v}(x, t) = \mathcal{F}_{\tau \rightarrow t} v(x, \tau) = \int_{\mathbb{R}} e^{-it\tau} v(x, \tau) d\tau.$$

We say that  $t$  is the pseudo-time corresponding to the complex frequency  $\tau$ .

The Fourier transform of the equation

$$\Delta v(x, \tau) + 2i\tau\eta \cdot \nabla v(x, \tau) + \left(\frac{1}{\sigma} \nabla \sigma\right) \cdot (\nabla + i\tau\eta) v(x, \tau) = 0.$$

is

$$\Delta \widehat{w}(x, t) + 2\eta \frac{\partial}{\partial t} \cdot \nabla \widehat{w}(x, t) + \left(\frac{1}{\sigma} \nabla \sigma\right) \cdot \left(\nabla + \eta \frac{\partial}{\partial t}\right) \widehat{w}(x, t) = 0.$$

The principal part of the equation

$$\Delta \hat{v}(x, t) + 2\eta \frac{\partial}{\partial t} \cdot \nabla \hat{v}(x, t) + \frac{1}{\sigma} (\nabla \sigma) \cdot (\nabla + \eta \frac{\partial}{\partial t}) \hat{v}(x, t) = 0$$

is given by the operator

$$\tilde{\square} = \mathcal{P}_R + i\mathcal{P}_I = \Delta + 2\eta \frac{\partial}{\partial t} \cdot \nabla$$

where  $\eta = \eta_R + i\eta_I$  and

$$\mathcal{P}_R = \Delta + 2\eta_R \frac{\partial}{\partial t} \cdot \nabla$$

$$\mathcal{P}_I = 2\eta_I \frac{\partial}{\partial t} \cdot \nabla$$

They have symbols

$$p_R(x, t, \xi, \tau) = \xi_1^2 + \xi_2^2 + 2\tau\eta_R \cdot \xi$$

$$p_I(x, t, \xi, \tau) = 2\tau\eta_I \cdot \xi$$

## Complex principal type operator

Let  $p(x, t, \xi, \tau) = p_R + ip_I$  be the symbol of  $\tilde{\square} = \mathcal{P}_R + i\mathcal{P}_I$ .  
The characteristic variety of  $p$  is

$$\Sigma = \{(x, t, \xi, \tau) \in T^*\mathbb{R}^3 \setminus 0; p(x, t, \xi, \tau) = 0\}.$$

On  $\Sigma$  the Poisson brackets of  $p_R(x, t, \xi, \tau)$  and  $p_I(x, t, \xi, \tau)$  satisfy

$$\{p_R, p_I\} = (\partial_x p_R \cdot \partial_\xi p_I + \partial_t p_R \cdot \partial_\tau p_I) - (\partial_\xi p_R \cdot \partial_x p_I + \partial_\tau p_R \cdot \partial_t p_I) = 0$$

and the differentials  $dp_R$  and  $dp_I$  are linearly independent on  $\Sigma$ .

This implies that  $\tilde{\square} = \mathcal{P}_R + i\mathcal{P}_I$  is a complex principal type operator.

## Propagation of singularities

By Hörmander-Duistermaat 1972, for a real principal type operator, e.g the wave operator  $\square_g$ , there are invertible Fourier Integral Operators  $A_1$  and  $A_2$  such that

$$\square_g = A_1 \frac{\partial}{\partial y_1} A_2, \quad (y_1, y_2, \dots, y_{2d}) \in \mathbb{R}^{2d}.$$

For the wave equation the light-like singularities propagate along light rays.

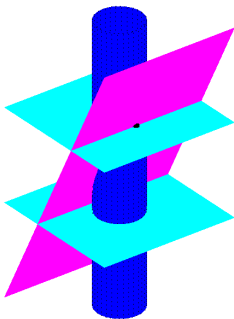
For the complex principal type operator  $\tilde{\square} = \mathcal{P}_R + i\mathcal{P}_I$  there are invertible Fourier integral operators  $A_1$  and  $A_2$  such that

$$\tilde{\square} = A_1 \left( \frac{\partial}{\partial y_1} + i \frac{\partial}{\partial y_2} \right) A_2, \quad (y_1, y_2, \dots, y_{2d}) \in \mathbb{R}^{2d}.$$

For  $\tilde{\square}$ , singularities propagate along two dimensional surfaces, called strips.

For example, if  $\tilde{\square}G(x, t) = \delta(x, t)$  then  $G(x, t)$  is singular on planes  $t = 0$  and  $2\eta_R \cdot x + t = 0$ .

In this talk, our aim is to consider propagation and reflection of singularities in Complex Geometric Optics.  
In figure below the magenta plane wave hits to the blue surface and causes reflected light blue waves.



Next we explain this in detail for equation  $\nabla \cdot \sigma \nabla u = 0$ .



## Outline:

- ▶ Inverse conductivity problem
- ▶ Motivation of the edge detection problem
- ▶ Complex principal type operators
- ▶ Beltrami equation
- ▶ Single scattering and connection to Radon transform
- ▶ Analysis of higher order terms

$$\bar{\partial}_z = \frac{1}{2}\left(\frac{\partial}{\partial x} + i\frac{\partial}{\partial y}\right), \quad \partial_z = \frac{1}{2}\left(\frac{\partial}{\partial x} - i\frac{\partial}{\partial y}\right), \quad z = x + iy \in \mathbb{C}$$

# Complex formulation of conductivity equation

We denote  $z = x_1 + ix_2 \in \mathbb{C}$  and identify  $\mathbb{R}^2$  with  $\mathbb{C}$ .

We use complex frequency  $k = \tau\theta$  where  $\tau \in \mathbb{R}$  and  $\theta \in \mathbb{C}$ ,  $|\theta| = 1$ .

In Astala-Päivärinta 2006, solutions for  $\nabla \cdot \sigma \nabla u = 0$  are written using the real-linear Beltrami equation,

$$\begin{aligned}\bar{\partial}_z f_\mu(z, k) &= \mu(z) \overline{\partial_z f_\mu(z, k)}, \quad z \in \mathbb{C}, \\ f_\mu(z, k) &= e^{ikz} (1 + \mathcal{O}(|z|^{-1})) \text{ as } |z| \rightarrow \infty.\end{aligned}$$

Here, the **Beltrami coefficient**  $\mu(z)$  is defined by

$$\mu(z) = \frac{1 - \sigma(z)}{1 + \sigma(z)}.$$

$\mu$  is supported in  $\Omega$  and  $\|\mu\|_{L^\infty(\mathbb{C})} < 1$ .

The function  $u = \operatorname{Re}(f_\mu) + i \operatorname{Im}(f_{-\mu})$  satisfies  $\nabla \cdot \sigma \nabla u = 0$ .

The map  $\Lambda_\sigma$  determines  $f_{\pm\mu}(z, k)$  for  $z \in \mathbb{C} \setminus \Omega$ .

# Notations

Let us write the Complex Geometrical Optics solutions of the Beltrami equation

$$\bar{\partial}_z f_\mu = \mu \overline{\partial_z f_\mu}$$

in the form of  $f =$  'incident wave' + 'scattered wave',

$$f_\mu(z, k) = e^{ikz} v(z, k),$$

$$v(z, k) = 1 + v_{sc}(z, k),$$

$$v_{sc}(z, k) = \mathcal{O}(|z|^{-1}), \quad \text{as } z \rightarrow \infty.$$

Let

$$e_k(z) = e^{i(kz + \bar{k}z)} = e^{i2\operatorname{Re}(kz)},$$

so that  $|e_k(z)| = 1$  and  $\overline{e_k(z)} = e_{-k}(z)$ .

The solid Cauchy transform  $\bar{\partial}_z^{-1}$  is

$$\bar{\partial}_z^{-1} f(z) = \frac{1}{\pi} \int_{\mathbb{C}} \frac{f(z')}{z - z'} d^2 z',$$

For any  $k \in \mathbb{C}$ , the scattered wave  $v_{sc}(z, k)$  satisfies

$$\bar{\partial}_z v_{sc} - \mu e_{-k} \overline{(\partial_z + ik)v_{sc}} = -i\bar{k} e_{-k} \mu, \quad v_{sc}(z, k) = \mathcal{O}(|z|^{-1})$$

that yields the Lippmann-Schwinger type equation

$$(I - \mathcal{A})v_{sc} = -i\bar{k} \bar{\partial}_z^{-1}(e_{-k} \mu),$$

where

$$\mathcal{A}v = \bar{\partial}_z^{-1}(e_k \mu \rho(\partial_z + ik)v)$$

and  $\rho(f) := \bar{f}$  denotes complex conjugation.

# Neumann series

Using  $(I - \mathcal{A})v_{sc} = -i\bar{k}\bar{\partial}_z^{-1}(e_{-k}\mu)$  we can write

$$v_{sc} \sim \sum_{n=1}^{\infty} v_n, \quad v_1 = -i\bar{k}\bar{\partial}_z^{-1}(e_{-k}\mu), \quad v_{n+1} = \mathcal{A}v_n.$$

More precisely,  $v_n$  is the  $n$ :th Frechet derivative of the map  $V_k : \mu \rightarrow v_{sc}(\cdot, k)$ , that is,  $v_n = D^n V_k|_0[\mu, \mu, \dots, \mu]$ .

Next we consider the term corresponding to [single scattering](#),

$$v_1 = -i\bar{k}\bar{\partial}_z^{-1}(e_{-k}\mu).$$

The Dirichlet-to-Neumann map  $\Lambda_\sigma$  determines  $v_{sc}(z, k)$  for  $z \in \partial\Omega$ .

The term  $v_1(z, k)|_{z \in \partial\Omega}$  determines singularities of  $\mu$ .

The terms  $v_n(z, k)|_{z \in \partial\Omega}$ ,  $n \geq 2$  contribute 'multiple scattering', which explain artifacts in numerics.

# Analysis of single order scattering in time domain

We use complex frequency  $k = \tau\theta$ ,  $\theta \in \mathbb{S}^1 = \{\theta \in \mathbb{C} : |\theta| = 1\}$   
and the Fourier transform

$$\mathcal{F}_{\tau \rightarrow t} w(z, t) = \int_{\mathbb{R}} e^{-it\tau} w(z, \tau) d\tau.$$

The Fourier transform of the single scattering term

$$v_1(z, t, \theta) = -i\bar{k} \bar{\partial}_z^{-1}(e_{-k}\mu),$$

is

$$\hat{v}_1(z, t, \theta) = \frac{2}{\theta} \int_{\mathbb{C}} \frac{1}{z - z'} \delta'(t + 2\operatorname{Re}(\theta z')) \mu(z') d^2 z'$$

# Generalised Radon transform

Define  $T_1 : \mathcal{E}'(\Omega) \rightarrow \mathcal{D}'(\partial\Omega \times \mathbb{R} \times \mathbb{S}^1)$  by setting

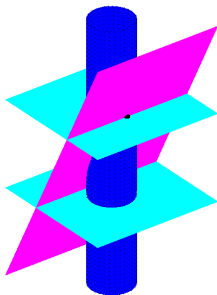
$$\mu(z') \mapsto (T_1\mu)(z, t, \theta) = \widehat{v}_1(z, t, \theta).$$

The Schwartz kernel of  $T_1$  is

$$K_1(z, t, \theta, z') = \left( \frac{2}{\theta} \frac{1}{z - z'} \right) \delta'(t + 2\operatorname{Re}(\theta z')).$$

For  $z \in \partial\Omega$  and  $z' \in \operatorname{supp}(\mu) \subset\subset \Omega$  the first factor is smooth. Hence  $T_1$  is a **generalized Radon transform** and thus a Fourier integral operator (**FIO**).

Consider the conductivity is  $\sigma(x) = 1 + \chi_{B(0,r_0)}(x)$  and fixed  $\theta$ .  
 Then  $(z, t) \mapsto \widehat{v}_1(z, t, \theta)$  is singular on three planes:

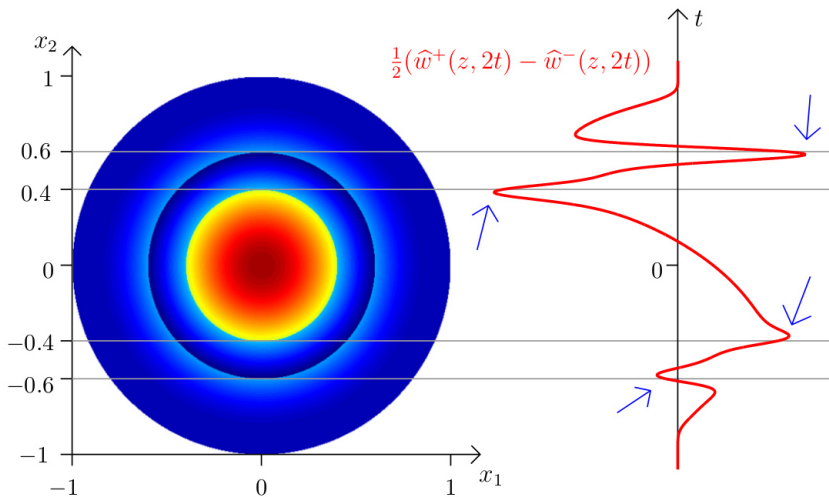


The magenta plane is the singsupp of the incident wave  $f_\theta(z, t) = c\delta(t + 2\text{Re}(\theta z))$ . We have  $\widehat{v}_1(z, t, \theta) = c\overline{\partial}_z^{-1}(\mu \cdot f'_\theta)$  where  $\overline{\partial}_z^{-1}$  propagates the singularities of the product  $\mu \cdot f'_\theta$ .



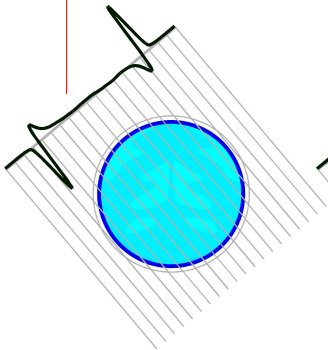
# Numerical results (with high resolution data)

Figure shows jumps of  $\sigma(z)$  and singularities of  $t \mapsto \widehat{v}_{sc}(z, t, \theta)$ .

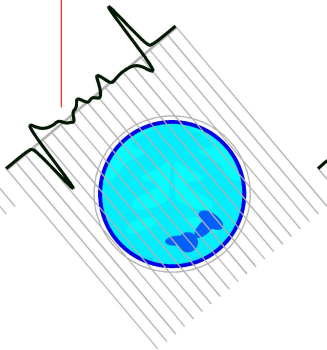


# 'X-ray images' appear in the EIT measurements

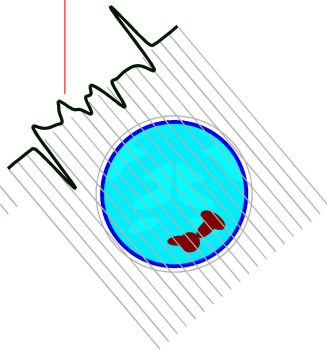
no jump



jump down



jump up



# The filtered back projection formula for EIT

Let us consider the 'complex average' of  $\widehat{v}_1(z, t, \theta)$  over  $z \in \partial\Omega$ ,

$$\widehat{v}_1^a(t, \theta) = \frac{1}{2\pi i} \int_{\partial\Omega} \widehat{v}_1(z, t, \theta) dz.$$

Let  $T_1^a$  be the operator  $T_1^a : \mu \mapsto \widehat{v}_1^a$ .

## Theorem

$(T_1^a)^* T_1^a \in \Psi^1(\mathbb{C})$  is a pseudo-differential operator with

$$\sigma_{prin}((T_1^a)^* T_1^a)(z, \zeta) = |\zeta|, \quad z \in \Omega$$

and

$$(2\pi)^{-\frac{1}{2}} (-\Delta)^{-\frac{1}{2}} (T_1^a)^* T_1^a = I \quad \text{mod } \Psi^{-1}(\Omega). \quad (2)$$

Formula (2) is analogous to the filtered back projection formula for Radon transform.

# Reconstruction algorithm

**Algorithm:** Given the Dirichlet-to-Neumann map  $\Lambda_\sigma$ , we determine  $\widehat{v}_{sc}(z, t, \theta)$ ,  $z \in \partial\Omega$  and

$$\widehat{v}_{sc}^a(t, \theta) := \frac{1}{2\pi i} \int_{\partial\Omega} \widehat{v}_{sc}(z, t, \theta) dz.$$

Then the reconstructed conductivity  $\sigma_{rec}(z)$  is

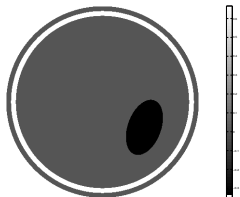
$$\begin{aligned} \mu_{rec}(z) &= (2\pi)^{-\frac{1}{2}} (-\Delta)^{-\frac{1}{2}} (T_1^a)^* \widehat{v}_{sc}^a, \\ \sigma_{rec}(z) &= \frac{1 - \mu_{rec}(z)}{1 + \mu_{rec}(z)}. \end{aligned}$$

On the level of single approximation the reconstructed conductivity  $\sigma_{rec}(z)$  has the same singularities as  $\sigma(z)$ .

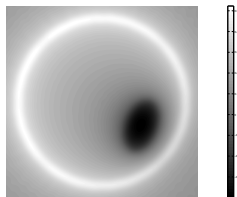
Below, we consider the effect of the higher order scattering.

# Numerical results (with high resolution data)

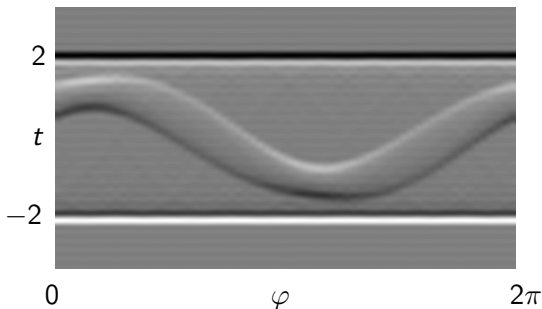
Phantom  $\sigma(x)$



Reconstruction from  $v_1$

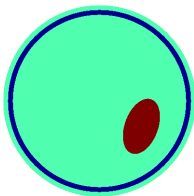


Sinogram of  $\hat{v}_1(z, t, \theta)$  'averaged' on  $z \in \partial\Omega$

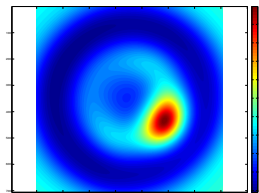


# Numerical results (Dirichlet-to-Neumann data)

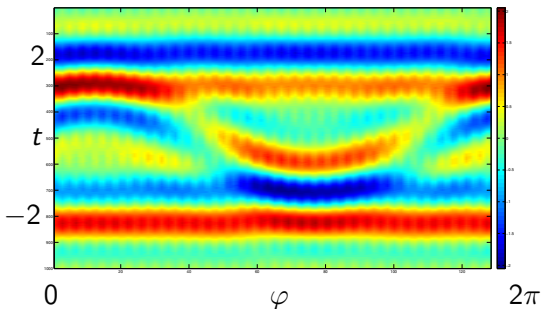
Phantom  $\sigma(x)$



Reconstruction from  $v_{sc}$



Sinogram of  $\hat{v}_{sc}(z, t, \theta)$  'averaged' on  $z \in \partial\Omega$

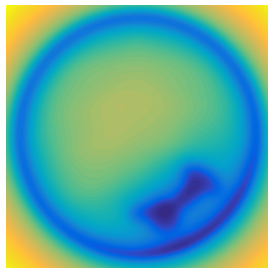


# Numerical results (with high resolution data)

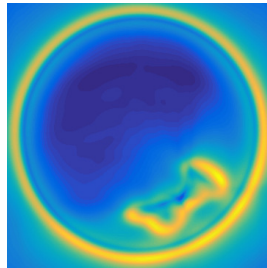
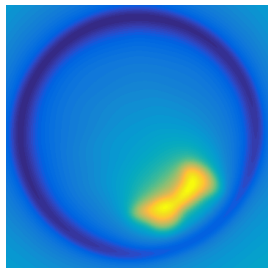
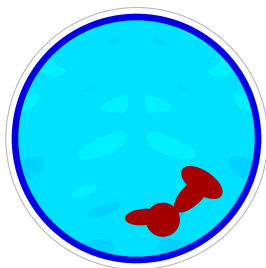
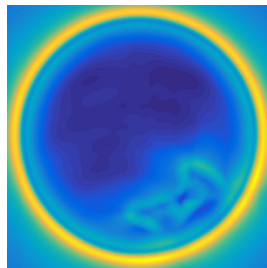
Conductivity



Filtered back-projection



$\Lambda$ -tomography



# Analysis of higher order terms in time domain

## Theorem

Assume that  $\sigma$  has jumps on smooth curves  $\gamma_j \subset \mathbb{R}^2$ ,  $j = 1, 2, \dots, J$  having non-zero curvature.

Then the wavefront set of  $\widehat{v}_{2n+1}$  consists of singularities of the plane wave that propagate along  $\text{char}(\mathcal{P})$  and reflect at most  $2n+1$  times from discontinuities of  $\sigma$ . Similar results hold for  $\widehat{v}_{2n}$ .

For example, when  $\text{singsupp}(\sigma) = \partial B(0, a)$ , we have

$$L_p = \{(z, t, \theta) \in \mathbb{R}^2 \times \mathbb{R} \times \mathbb{S}^1\} : t = 2ap\}, \quad \text{for } p \in \mathbb{Z}.$$

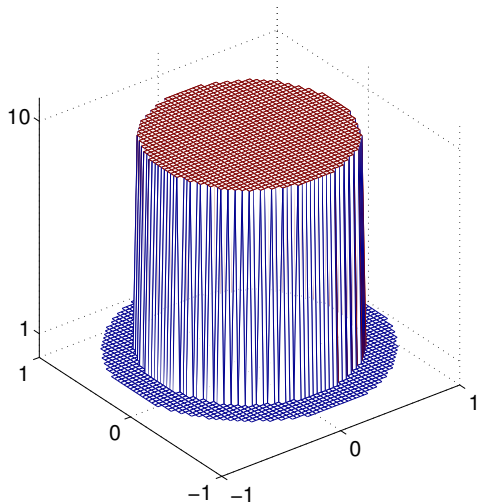
Outside the support of  $\mu(z)$ , we see that

$$\text{singsupp}(\widehat{v}_{2n+1}) \cap \{(z, t, \theta); |z| \geq 1\} \subset \bigcup_{p=1}^n (L_{2p-1} \cup L_{-(2p-1)}).$$



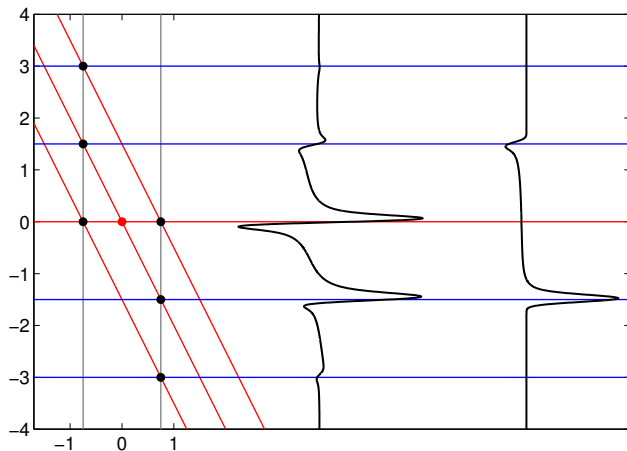
## Numerical results for $\sigma(x) \in [1, 10]$

Let us consider  $\sigma(z)$  having large jumps.

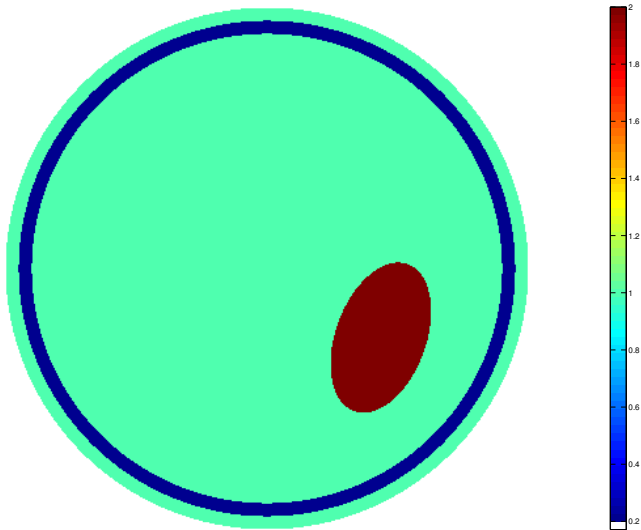


# Numerical results for $\sigma(x) \in [1, 10]$

Geometry of the singularities of  $\hat{1} + \hat{v}_1 + \hat{v}_2$ , and functions  $t \mapsto \hat{v}(z, t, \theta)$  and  $t \mapsto \hat{v}_1(z, t, \theta)$ .

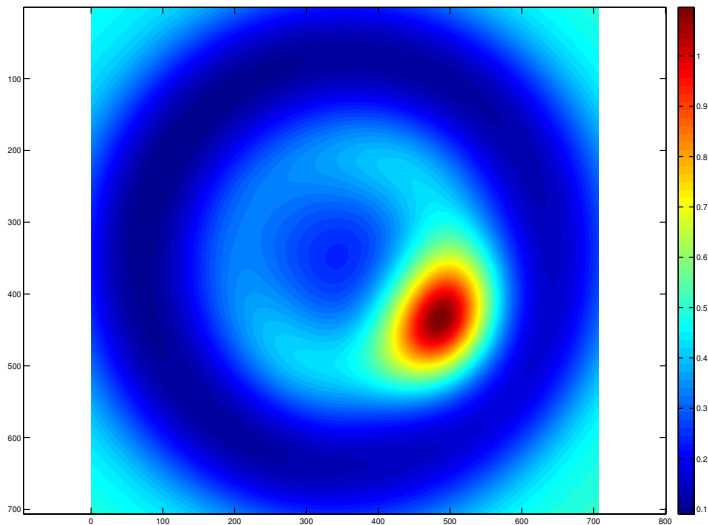


Numerical results for  $\sigma(x) \in [0.5, 2]$



The model object.

# Numerical results for $\sigma(x) \in [0.5, 2]$



The reconstruction, no artefacts from higher order terms are visible.

Thank you for your attention!